9 Cuprate Superconductors

The discovery of so-called *high-temperature superconductors* by Johannes Georg Bednorz and Karl Alexander Müller in 1986 marked the beginning of a new era in the field of superconductivity. The two had found a sudden decrease in electrical resistance by at least three orders of magnitude in compounds of barium (Ba), lanthanum (La), copper (Cu) and oxygen (O) with falling temperature. The drop had started at about 35 K, and it was suspected that this was a new type of superconductivity. However, since superconductivity started at temperatures up to 12 K higher than the record critical temperature of 23.2 K for the compound Nb_3Ge, which had been in existence for 12 years at the time, caution and skepticism were called for.

In the case of Bednorz and Müller, however, the period of skepticism did not last long, as their results were already confirmed at the end of 1986. In 1987, Paul Ching-Wu Chu and colleagues reported a sensational progress: In a modification of the original oxides, in which the larger lanthanum atom was replaced by the smaller yttrium atom, they observed the enormous increase in the critical temperature up to 92 K. The critical temperature of 92 K of this recently discovered new material $YBa_2Cu_3O_7$ (abbreviated YBCO) is even significantly higher than the boiling temperature of 77 K for liquid nitrogen. Now the relatively expensive liquid helium as coolant could be replaced by the much cheaper liquid nitrogen.

An overview of the time course of the discovery of the different superconductors with their critical temperature T_C is shown in Fig. 9.1.

The new class of "cuprate superconductors" (Fig. 9.2) consists of oxides with perovskite structure. They are composed of copper oxide (CuO_2) planes in which the copper and oxygen atoms form a two-dimensional lattice. The crystallographic unit cells of each compound contain a different number of copper oxide planes. A distinction is made between five main families of cuprate superconductors, whose "progenitors" and critical temperatures T_C are listed in Table 9.1.

R. P. Huebener, *History and Theory of Superconductors,* Springer essentials,
https://doi.org/10.1007/978-3-658-32380-6_9

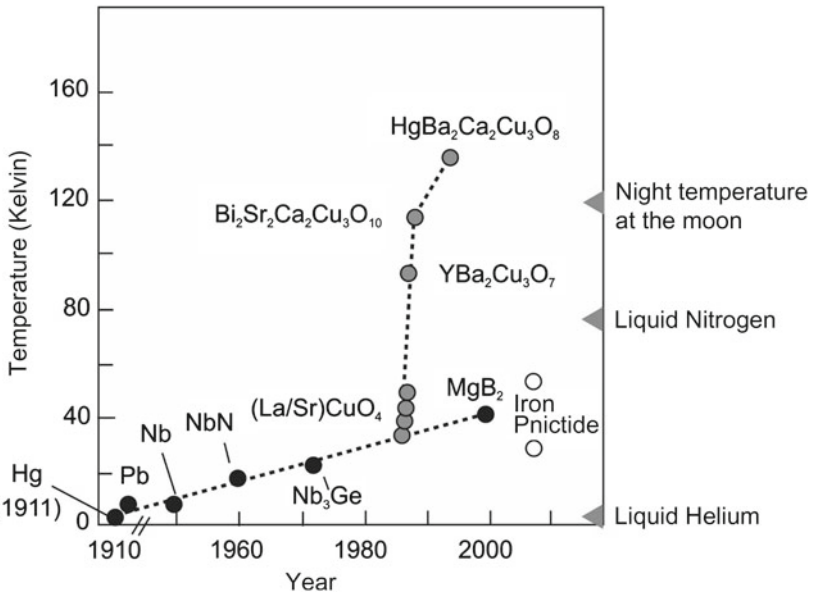

Fig. 9.1 Critical temperature T_C plotted over the year of discovery of various superconductors. The steep curve branch on the right shows some high temperature superconductors. (R. Kleiner)

The copper oxide planes of the cuprates determine the electrical and especially the superconducting properties. Doping with electrical charge carriers plays an important role in this process. In the undoped state, the cuprates are initially electrical insulators. The elementary magnets of the copper atoms in the CuO_2 planes are alternately oriented in opposite directions (antiferromagnetism). Superconductivity only occurs when the electron concentration in the CuO_2 planes is reduced by *doping with holes.* For example, this hole doping is caused by the extraction of oxygen. However, superconductivity only occurs in a relatively narrow concentration range of the doping, so that the oxygen concentration must be carefully controlled during material preparation. Table 9.1 shows the critical temperature values for the case of optimum hole doping. The highest critical temperature value observed so far at normal pressure, $T_C = 133$ K, was found in the compound $HgBa_2Ca_2Cu_3O_{8+x}$. At high pressure, this compound even shows a critical temperature of 164 K.

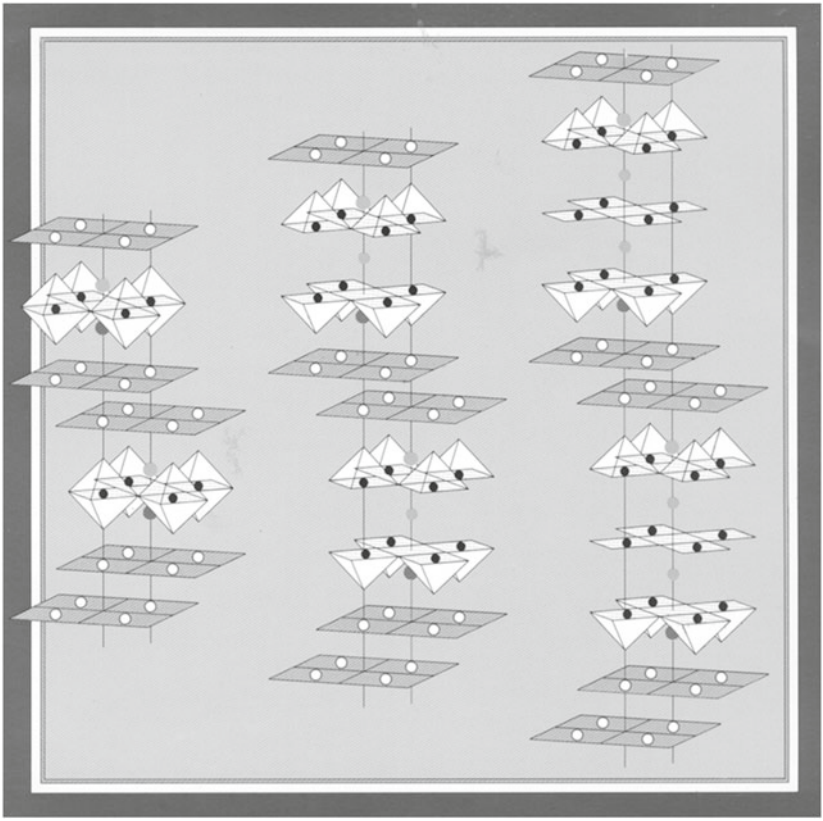

Fig. 9.2 Crystal structure of different cuprate superconductors. At the 6 corners of the light octahedrons or at the 5 corners of the light pyramids, there are oxygen atoms. The centers of the octahedrons or the base of the pyramids are occupied by copper atoms (IBM)

Table 9.1 Critical temperatures of various high-temperature superconductors

Compound	T_C (K)
$La_{2-x}Sr_xCuO_4$	38
$YBa_2Cu_3O_{7-x}$	92
$Bi_2Sr_2CaCu_2O_{8+x}$	110
$Tl_2Ba_2Ca_2Cu_3O_{10+x}$	125
$HgBa_2Ca_2Cu_3O_{8+x}$	133

In contrast to doping with holes, *doping with electrons,* i.e., with negative charges, is necessary for superconductivity in some compounds. However, the concentration range of the doping required for superconductivity is lower in this case and the critical temperature is significantly lower than for compounds doped with holes.

As expected, the layered crystal structure of the cuprate superconductors with its structure of the CuO_2 planes (Fig. 9.2) causes a strong dependence of the electrical and thermal transport properties on the crystal direction. The electrical resistivity in the normal state perpendicular to the CuO_2 planes is up to several orders of magnitude higher than parallel to these planes. In the normal state of the cuprates, the temperature dependence of the electrical resistance, the Hall effect, as well as the Seebeck and Peltier effect, shows a behavior that clearly differs from that of metals.

Soon after the discovery of high-temperature superconductors, it was recognized that the coherence length ξ, which characterizes the spatial rigidity of the superconducting properties, is much smaller in these materials than in classical superconductors. Its size is in the range of the dimensions of the crystallographic unit cell. This leads to a particularly high sensitivity to atomic defects and grain boundaries. Since the coherence length also determines the extent of the core of the magnetic flux lines (see Fig. 5.3), atomic defects and grain boundaries already act as pinning sites for magnetic flux quanta. From the density of the condensation energy of Eq. (2.4), we can see that per unit length of the magnetic flux line, the condensation energy $\left(H_C^2/8\pi\right)\pi\xi^2$ has to be provided for the normal nucleus. This energy can be saved in whole or in part if the core of the flux line passes through a region of the superconductor in which superconductivity is already suppressed by the material inhomogeneity of a pinning center.

The granular structure and spatial inhomogeneity of cuprate superconductors was initially a difficulty that had to be overcome if technical applications of these materials were to be realized. In Fig. 9.3, we show an early example using one of the first prepared thin films of the cuprate superconductor $Y_1Ba_2Cu_3O_7$ with further explanations in the legend.

In the case of cuprate superconductors, the question of whether the formation of Cooper pairs is the central mechanism for superconductivity, as in classical superconductors, could be clarified early on. The positive answer was found from the size of the magnetic flux quantum and the relation between electric voltage and frequency in the Josephson effect, where the double elementary charge of the Cooper pairs always occurred. However, the microscopic pairing mechanism of the cuprates has not yet been clarified.

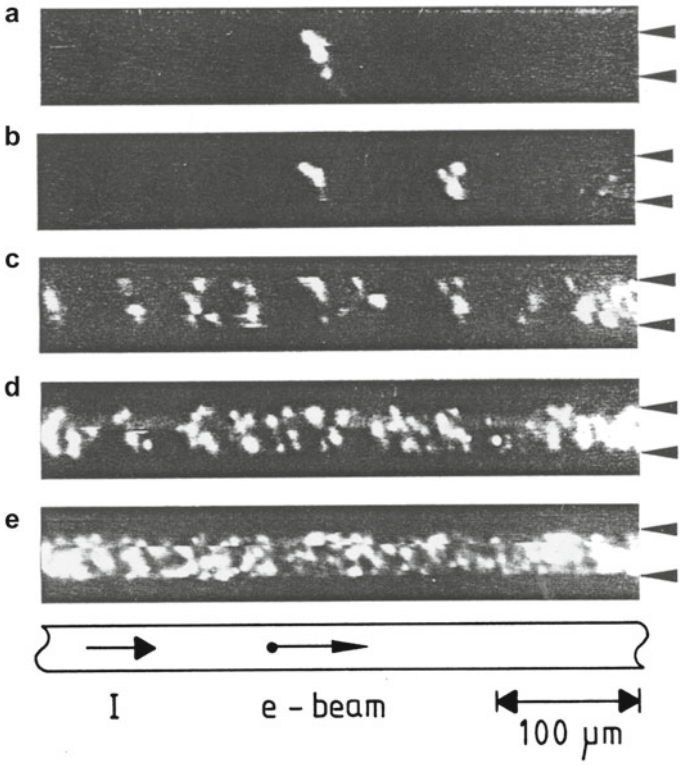

Fig. 9.3 Granular structure of one of the first prepared thin films of the cuprate superconductor $Y_1Ba_2Cu_3O_7$. The layer running horizontally in the figure has a width of 30 μm. The arrowheads on the right mark the upper and lower edges of the layer. Bright spots indicate the locations where electrical resistance occurs in the layer when exposed to electrical current. The dark areas are superconducting. In the series of figures (a) to (e), the electrical current was successively increased from 0.7 mA at (a) to 8.7 mA at (e). The figures show the strong spatial inhomogeneity of the layer with large fluctuations in the local critical electrical current density. The figures were taken using the method of low temperature scanning electron microscopy. The temperature was 53 K

The upper critical magnetic field H_{C2} in cuprate superconductors is up to more than 100–200 times greater than the highest values in classical superconductors. This can be understood using the Ginzburg–Landau theory and the extremely small values of the coherence length.

9.1 Symmetry of the Wave Function

With the reference to the Ginzburg–Landau theory in Chap. 5 and to the BCS theory in Chap. 6, we had presented the macroscopic wave function (Eq. (5.1)) to describe the state of the superconducting electrons. In the case of the cuprate superconductors, we have to discuss especially the symmetry of this wave function. In classical superconductors, the wave function is generally isotropic (s-wave symmetry). In the case of the cuprates, however, the layer structure with the CuO_2 planes must already be taken into account. To illustrate the symmetry of the wave function, a representation in the momentum space is useful. In the two-dimensional **k**-space, which is spanned by k_x and k_y, the amplitude of the wave function is plotted as a function of direction.

In the case of hole-doped high-temperature superconductors, the wave function shows a strong directional dependence, which is determined by the atomic d-orbitals of the copper atoms in the CuO_2 planes. In Fig. 9.4, we show the polar plot of the amplitude of the wave function in two-dimensional **k**-space with the four lobes of the d-orbitals. As a function of the polar angle, we can see the nodes and antinodes as well as the alternating sign. The crystallographic arrangement of the nodes and antinodes is shown for the case of $d_{x^2-y^2}$ symmetry. The isotropic case with s-wave symmetry is also shown for comparison. To identify the directions of the nodes and antinodes, we show in Fig. 9.5 the case of the square CuO_2 lattice in the CuO_2 planes.

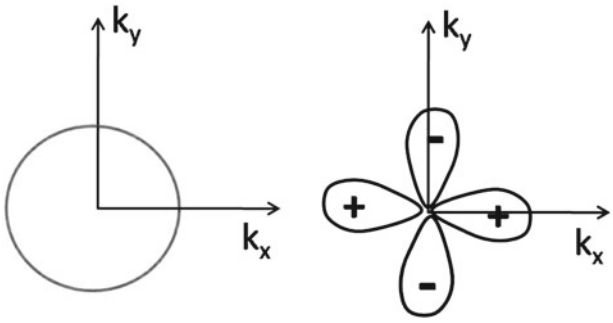

Fig. 9.4 Representation of the wave function with s-wave symmetry (*left*) and with $d_{x^2-y^2}$ symmetry (*right*) in **k**-space (k_x–k_y plane). The latter symmetry dominates in the CuO_2 planes of the cuprate superconductors

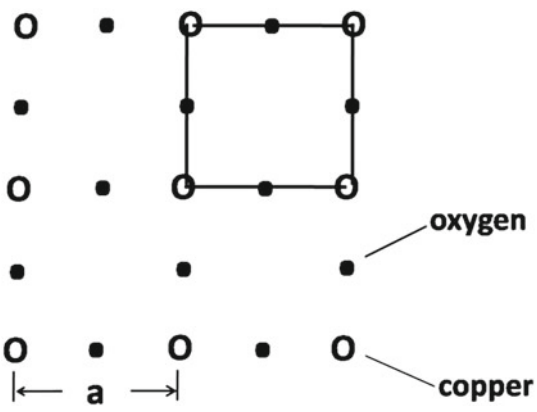

Fig. 9.5 Scheme of the square CuO_2 lattice. The unit cell is marked with the solid line. The lattice constant a is indicated

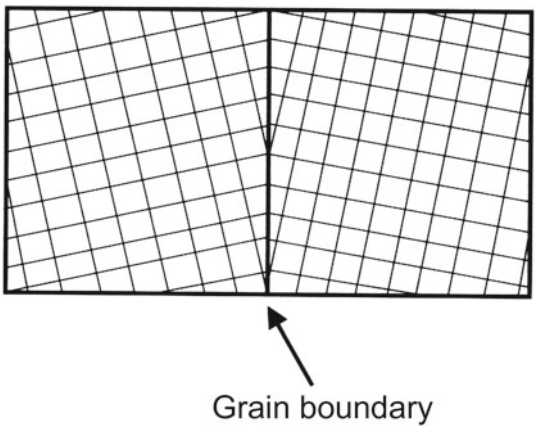

Fig. 9.6 Bicrystal technique for controlled preparation of a single grain boundary in a cuprate superconductor layer. An artificially produced bicrystal is used as substrate, in which two differently oriented monocrystalline parts are separated from each other by an atomically sharp grain boundary. The grain boundary in the substrate is then transferred exactly to the superconductor layer prepared above it. On both sides of the grain boundary, there are monocrystalline superconductor layers with different crystal orientation

The change of sign of the wave function when moving around the coordinate origin in the plane k_x–k_y and the four zero-crossings of the amplitude at the nodes have significant effects on the superconducting properties of materials with d-wave symmetry. The energy gap disappears at the nodes and increases again on both sides.

9.2 Vortex Matter

The layered structure of the cuprate superconductors with the superimposed CuO_2 planes has strong effects on the vortex lattice in the superconducting mixed state. Here we limit ourselves to the case where the magnetic field is oriented perpendicular to the CuO_2 planes. The magnetic flux lines now consist of single small disks, since the superconducting property is limited to the CuO_2 planes. These disks are also called *pancakes*. Due to this decomposition of the individual flux lines, the vortex lattice has numerous new properties. In the literature, this novelty is summarized under the term *vortex matter*. For example, individual disks can now leave their stacked arrangement, which can be regarded as melting and evaporation of the vortex matter.

The new properties of vortex matter are particularly evident in the electrical resistance behavior and electrical losses. As we discussed in Chapter 8, the movement of the magnetic flux lines under the influence of the Lorentz force is the main cause of the electrical losses. This becomes all the more serious when individual parts of the magnetic flux lines can already start moving as small disks. The installation of effective pinning centers is therefore of particular importance. Due to the small coherence length of the cuprates, pinning centers on an atomic length scale, such as missing oxygen atoms in the CuO_2 planes and grain boundaries, are already effective here.

9.3 Grain Boundaries

The granular structure of the oxide cuprate superconductors with their numerous grain boundaries was a great challenge from the very beginning, since superconductivity is generally interrupted within the grain boundaries. The task was therefore to reduce the number of grain boundaries as far as possible. Furthermore, the physical properties of the grain boundaries had to be clarified.

With the help of the already highly developed thin-film technology, it was soon possible to produce monocrystalline thin films of the high-temperature superconductors on suitable substrates. Critical electrical current densities of more than 1 million A/cm^2 could already be achieved at the boiling temperature of liquid nitrogen of 77 K.

The so-called "bicrystal technique" has proven to be very useful for the investigation of grain boundaries. It is based on the following fact. During the epitaxial growth of the high-temperature superconductor layer, the crystal orientation of the monocrystalline substrate is transferred exactly to the superconductor layer above it. If a specially prepared bicrystal is used as a substrate, in which an atomically sharp grain boundary separates two differently oriented crystal regions from each other, then the grain boundary of the substrate is transferred exactly to the superconductor layer prepared above it. In Fig. 9.6, we show the schematic representation of a bicrystal. This bicrystal technique has proved to be very successful in many experiments. In particular, it is very successful in realizing the Josephson effect in high-temperature superconductors. Today, the bicrystal technique is widely used in the fabrication of Superconducting Quantum Interference Devices (SQUIDs) (see Sect. 12.1) based on high-temperature superconductors.

At the end of this section, we will discuss the special case where the bicrystal technique is used to fabricate an arrangement in which two lobes of the superconductor d-wave function meet with different signs. This arrangement is called "π contact". If such a π contact is built into a closed superconducting ring, there is so-called frustration, where the unambiguity of the wave function is destroyed. (A change of sign of the wave function remains after a complete revolution.) In this case, the frustration is cancelled by the spontaneous generation of a half-integer magnetic flux quantum.

In a famous experiment, Chang C. Tsuei and colleagues used this technique to prove the d-wave symmetry of the Cooper pair wave function for the high-temperature superconductors doped with holes. In Fig. 9.7, we show their result. They used a tri-crystal as substrate, in which three monocrystalline regions are arranged in such a way that at one of the three grain boundaries created, a sign change of the wave function occurs between the two sides, thus resulting in a π contact. The frustration is removed by spontaneously forming an exactly half numbered magnetic flux quantum at the common meeting point of the three grain boundaries. The half-integer magnetic flux quantum could be detected with a SQUID scanning microscope.

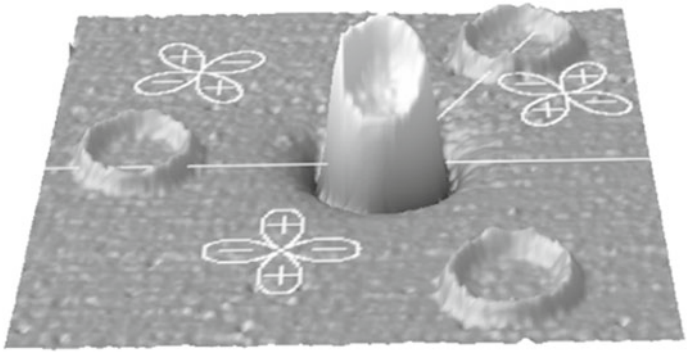

Fig. 9.7 Tri-crystal experiment by Tsuei to prove the d-wave symmetry of the quantum mechanical Cooper pair wave function in the cuprate superconductor $Y_1Ba_2Cu_3O_7$. The substrate is an artificially produced tri-crystal in which three differently oriented monocrystalline crystal parts are separated by atomically sharp grain boundaries. This crystal structure with its grain boundaries is transferred exactly to the superconductor layer prepared above. The grain boundaries are marked by the straight white lines. In the three crystal parts separated by the grain boundaries, the differently oriented d-wave symmetry of the Cooper pair wave function is indicated by the white four-leaf figures. A total of four superconducting rings have been fabricated from the YBaCuO layer at various locations, while the remaining part of the layer has been removed. The orientations of the three crystal parts are chosen in such a way that if d-wave symmetry of the wave function is present, an exactly half-integer magnetic flux quantum is spontaneously generated in the ring around the common meeting point of the three crystal parts, while nothing happens in the remaining three rings. The figure was obtained using a SQUID scanning microscope and shows the half-integer magnetic flux quantum in the middle ring around the common meeting point of the three crystal parts. The other rings remain only weakly indicated (C. C. Tsuei)

9.4 Intrinsic Josephson Contact

The layer structure of the cuprate superconductors with the superconducting CuO_2 layers, which are separated from each other by weakly conducting intermediate layers, suggests that there should be an "intrinsic Josephson effect" here. Reinhold Kleiner and Paul Müller were the first to prove the intrinsic Josephson effect in 1982. Here, several hundred to several thousand Josephson contacts are stacked on top of each other. Initially, Kleiner and Müller used small $Bi_2Sr_2CaCu_2O_8$ (BSCCO) single crystals that were clamped between two contact pins. This allowed an electric current to be passed through the crystal perpendicular to the CuO_2 planes. As soon as an electrical voltage appeared at the contacts above a critical

current level, a high-frequency Josephson alternating current was observed, according to the second Josephson Eq. (7.2), by means of the emitted microwaves. The emitted power of the electromagnetic radiation could be detected because it increases proportionally to the square of the large number of synchronously oscillating Josephson contacts stacked on top of each other in the crystal.

In the meantime, this technique has been further developed. Today, BSCCO towers, so-called "mesas," are used, which are manufactured on a substrate and carry an electrical contact. The principle is shown in Fig. 9.8. The technique is of particular interest as a source of radiation for microwaves in the frequency range 0.5–2 THz, as this frequency range has only been developed to a limited extent so far. Currently, microwave powers of several tens of μW are achieved in the terahertz range for individual mesas. Attempts are being made to increase this power even further by synchronizing networks of several mesas.

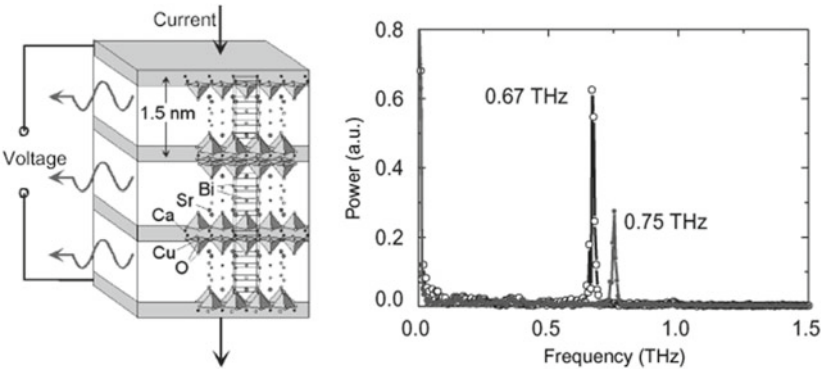

Fig. 9.8 Intrinsic Josephson contact as microwave source. (*Left*) Diagram of a stack of three Josephson contacts of a superconducting $Bi_2Sr_2CaCu_2O_8$ (BSCCO) crystal. The (dark drawn) copper oxide planes run through the base of the CuO pyramids. (*Right*) Emitted microwave spectrum of a BSCCO crystal (R. Kleiner)